Concept, Modeling and Fabrication Techniques for Large-Stroke Piezoelectric Unimorph Deformable Mirrors

Eui-Hyeok Yang*[a], Kirill Shcheglov[a] and Susan Trolier-McKinstry[b]

[a] Jet Propulsion Laboratory, California Institute of Technology
4800 Oak Grove Drive, Pasadena, CA 91109
* Eui-Hyeok.Yang@jpl.nasa.gov ph: +1-818-354-7059 fx: +1-818-393-6047

[b] The Pennsylvania State University
151 Materials Research Laboratory, University Park PA 16802

ABSTRACT

Large-stroke micromachined deformable mirror technology can boost the imaging performance of an otherwise non-rigid, lower-quality telescope structure. The proposed deformable mirror concept in this paper combines a microfabricated large-stroke piezoelectric actuator with a reflective membrane "transferred" in its entirety from a separate wafer. This process allows the large-stroke actuation of the continuous membrane and can provide the necessary large wavefront correction. The micromachined deformable mirror approach allows mass-production of actuators as well as scalable structures with, high actuator densities. The piezoelectric unimorph actuator design approach delivers large actuator stroke with a highly localized influence function, while maintaining a surface figure of optical quality. Both of these component fabrication techniques are easily scaled to accommodate deformable mirrors with very large areas.

Keywords: Deformable Mirror (DM), Microelectromechanical Systems (MEMS), Adaptive Optics (AO), Piezoelectric Actuator, Unimorph Membrane, Continuous Mirror, Wafer-Scale Membrane Transfer

1. INTRODUCTION

Ultra-large, lightweight space telescopes are envisioned by NASA for the scientifically critical UV-visible (0.1 μm - 1μm), mid-infrared (3-30 μm) and far-infrared (30-300 μm) wavelength regimes. Deploying conventional, rigid primary mirrors in space is prohibitively expensive. Therefore, it is planned to construct telescopes with either segmented apertures or with relatively flexible monolithic primary mirrors whose large surface errors can be corrected using subsequent active or adaptive wavefront control [1]. These concepts could potentially involve wavefront errors greater than several wavelengths. Thus, the key optical component needed for effective wavefront compensation is a large-stroke, continuous-membrane, deformable mirror with high actuator density over large areas.

Electrostrictive lead magnesium niobate (PMN) devices have achieved a surface stability of 1 angstrom and a surface figure of λ/20 [2]. Other materials, such as super-piezoelectric (PMN-PT) and lead zirconium titanate (PZT) ceramics, have also been developed for this application. Some of these materials have shown good cryogenic properties. However, although these technologies are in widespread use, they have only limited actuator stroke (approximately 0.5 μm stroke at 1/mm^2 actuator density, for PMN-based mirrors). MEMS-based designs, therefore, offer the potential of being highly scalable and achieve high pixel counts, while at the same time being highly cost effective. Although segmented deformable mirrors have been fabricated with tip/tilt capability on individual pixels [3, 4], a continuous surface figure is required to increase imaging sensitivity and avoid undesirable diffraction effects. Micromachined continuous membrane deformable mirrors have been fabricated [5-9]; however, such devices still have limited actuator stroke (< 6 μm for at 1/mm^2 actuator density), and with marginal surface quality. Current, large-aperture technology developments under the recent Gossamer program have yet to demonstrate the potential for

diffraction-limited wavefront quality over large apertures. Therefore, there exists a pressing need for a large-actuator-stroke deformable mirror to correct the large wavefront errors associated with flexible space-based telescope apertures. The approach described in this paper, will simultaneously meet the dual requirements of high optical quality (λ /20 at λ = 0.5 μm) and large stroke (> 6 μm at 4/mm^2 actuator density or > 30 μm at 0.1/ mm^2 actuator density), and is based on a large-stroke unimorph piezoelectric actuator technology combined with an optical-quality membrane transfer technology.

2. UNIMORPH DEFORMABLE MIRROR CONCEPT

The proposed deformable mirror consists of a continuous membrane mirror transferred onto arrays of piezoelectric unimorph actuators. The primary benefit of piezoelectrically actuated MEMS is precision spatial control, which more than offsets the added complexity of microfabrication. Recent studies indicate promising piezoelectric properties for thin-film material compositions [10]. Pixelated PZT actuated mirror arrays have been commercially developed [11]. The unimorph actuation principle is illustrated in Figure 1. A voltage applied to the piezoelectric layer induces lateral strain, which, because of the doubly clamped configuration, is converted to a vertical deflection of the unimorph. The vertical deflection causes the film to deform and pull on the mirror attached to it. The advantage of this approach is that the small strains obtainable at modest voltages from a piezoelectric material are converted into large vertical mirror displacements. In our current design, for a 500 μm actuator spacing, an approximately 6 μm vertical displacement is expected. In our previous experiments, at 77 °K, the actuation displacements of PZT films with a composition optimized for room temperature operation, dropped to ~25% of the room temperature value. Thus, optimization of the actuator material composition for operation at the required temperature ranges will have to be performed in the future. This could be accomplished, for instance, by choosing compositions with low ferroelectric transition temperatures (curie temperatures). Several options exist for this choice, including moving to a Zr-rich PZT or to related compositions with low transition temperatures, such as lead magnesium tungstate – lead titanate or lead magnesium tantalate – lead titanate.

3. MODELING OF PIEZOELECTRIC UNIMORPH MEMBRANES

Mathematical modeling was performed for piezoelectric unimorph (rectangular membrane geometry) with variable dimensions and clamped around the perimeter. The modeling approach involved the following steps:

a) Selection of a functional form with a proper choice of coordinates for the displacement vectors.
b) Calculation of the resulting strain distributions.
c) Integration of the differential elastic and piezo-elastic energy contributions over the actuator volume in order to obtain the total piezo-elastic energy for the configuration.
d) Minimization of the energy under the applied constraints (e.g. displacements being zero along the membrane edge) in order to obtain the membrane profiles for the various piezoelectric layer dimensions and applied voltages.

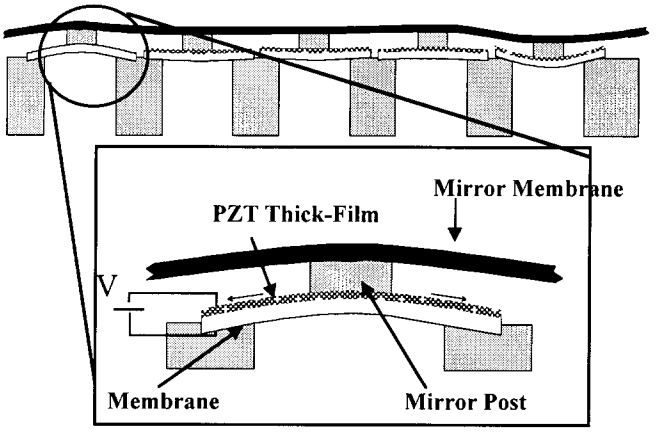

Figure 1: Thick-film piezoelectric unimorph based deformable mirror concept. A compliant, optical quality, single face-sheet mirror membrane is backed by an array of micro actuators. A voltage applied to the piezoelectric layer induces stress in the longitudinal direction causing the film to deform and pull on the mirror connected to it. The advantage of this approach is that the small strains obtainable from a piezoelectric material at modest voltages are translated into large displacements.

A set of constraints is included into the energy minimization calculation using a polynomial displacement function and the method of Lagrange multipliers. These constraints include both the actuator clamping around the perimeter and the central actuator displacement. Taking partial derivatives with respect to all the unknown coefficients of terms in the polynomial generates a set of linear equations. The resulting system of linear equations is solved numerically to obtain the relevant coefficients for the unimorph actuator profile and the vertical displacements at the center for various sets of initial conditions, such as the membrane dimensions, membrane thickness, materials properties, applied voltages, and normal forces. These coefficients are then substituted into the original form of the displacement function to obtain the membrane profiles corresponding to particular sets of initial conditions.

For the instance of a 500 μm × 500 μm unimorph actuator membrane, three different cases are considered; 16 μm thick Si, 26 μm thick Si, and 2 μm thick Si_3N_4 assuming a constant field of 10 kV/cm. Figure 2 shows the displacements for various values of PZT dimensions and PZT thickness for the three cases.

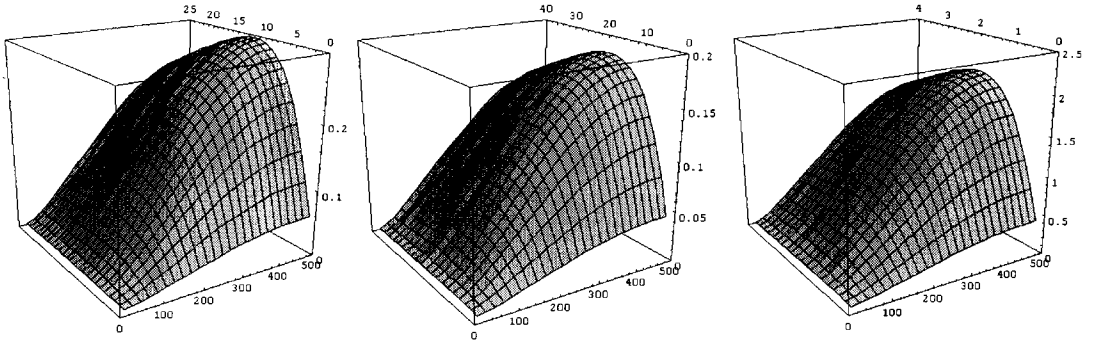

16 μm thick Si *26 μm thick Si* *2 μm thick Si_3N_4*

Figure 2: 3D plots of displacement vs. electrode lateral dimensions and the thickness. (All numbers are in μm.)

Via this calculation, the optimal electrode sizes are found to be 500 μm × 500 μm × 12.1 μm thick PZT for the 16 μm thick Si support membrane, 500 μm × 500 μm × 19.7 μm thick PZT for the 26 μm thick Si support membrane, and 480 μm × 480 μm × 2.1 μm thick PZT for the 2 μm thick Si_3N_4 support membrane. Subsequently actuator deflections at the center were calculated using these optimal parameters for the three membranes for various voltage and normal force conditions. These results are presented in Figure 3.

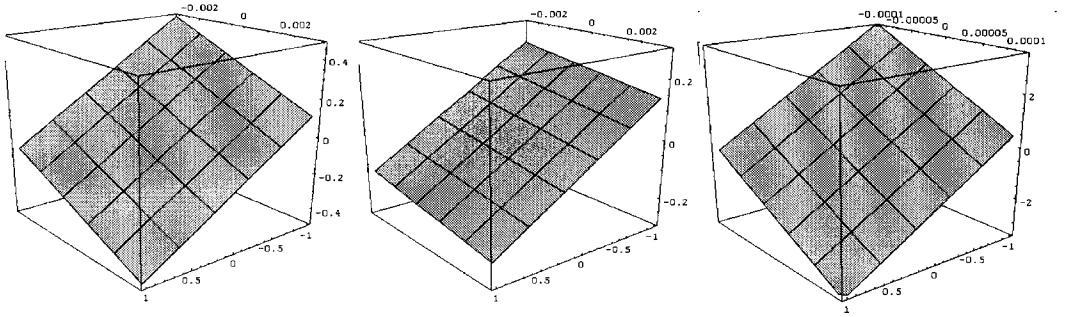

16 μm thick Si *26 μm thick Si* *2 μm thick Si_3N_4*

Figure 3: 3D plots of center displacement of unimorph actuator vs. applied voltage (-1V/μm to +1V/μm) and normal force (N).

Figure 4 shows the free (optical membrane not mounted) actuator center displacement for the case of Si $_3N_4$ membrane-based unimorph actuators as a function of the lateral membrane dimension. The lateral PZT electrode dimension is chosen to be 80% that of the Si_3N_4membrane, as this has been determined to be very close to optimum

size for achieving maximum deflection. The data is generated for 1.5 μm thick 6H PZT on 2 μm Si_3N_4 at 1V/μm applied field.

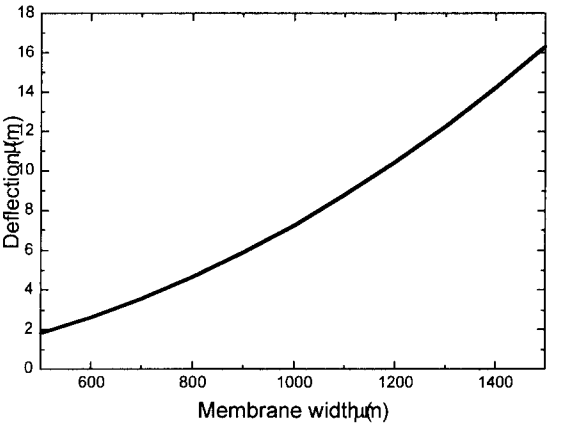

Figure 4: Actuator displacement at constant field vs. actuator size.

The deflection of the mirror membrane is modeled using the same principles used for modeling the piezo unimorph actuation. A set of basis functions for the displacement vectors is chosen (in this case a discrete Fourier expansion is selected due to the fact that the integration volume encompasses the entire mirror membrane, and thus one can take advantage of significantly simplified resulting equations). Strains are calculated, the elastic energy is integrated over the volume and subsequently minimized using the standard constrained minimization approach (Lagrange multipliers). In the case of the mirror membrane, as opposed to the actuator case, the boundary is unconstrained while an array of points within the membrane corresponding to the attachment points to individual actuators is constrained to be at the nominal actuator height. We also include the height/applied field/restoring force relationship for each actuator as a set of complementary equations. The relevant coefficients are taken from the previously completed piezo unimorph analysis and are reduced to two parameters, the field coefficient, c_e, and the force coefficient, c_f. These equations have the following form.

$$h_i = -c_e E_i - c_f F_i \qquad (1)$$

where E_i and F_i are applied fields and restoring forces, respectively, and h_i are the actuator displacements. Thus the resulting set of equations can be solved either to determine membrane profiles as a function of applied voltages, or to determine the set of applied voltages for the desired actuator displacements. The latter solution set is necessary for implementing control loops. Figure 5 shows the mirror surface profile, when a single actuator is turned on while the other surrounding actuators are turned off (for a 4 x 4 array of Si_3N_4 membrane-based unimorph actuators under a 2 mm wide, 5 μm thick Si optical membrane).

Figure 6 shows the mirror membrane profile obtained by requiring that all actuator displacements be zero except for one, which provides a 1 μm displacement The plot shows membrane displacement as a function of the applied electric fields required to achieve this membrane profile. Thus, this case illustrates the possibility of controlling the actuator array in order to obtain arbitrary membrane profiles. This task, however, is not trivial and a control algorithm based on the mathematical model must be developed.

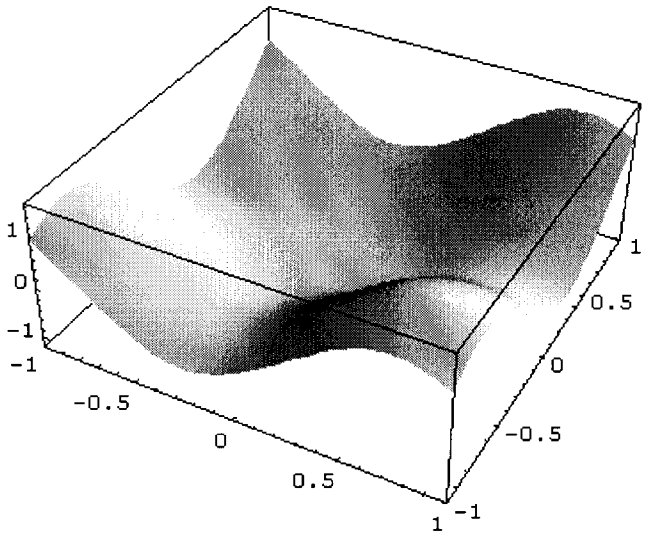

Figure 5: Membrane profile with one actuator at 1 V/μm, all others at 0 V/μm. (Vertical scale is in microns, lateral in mm)

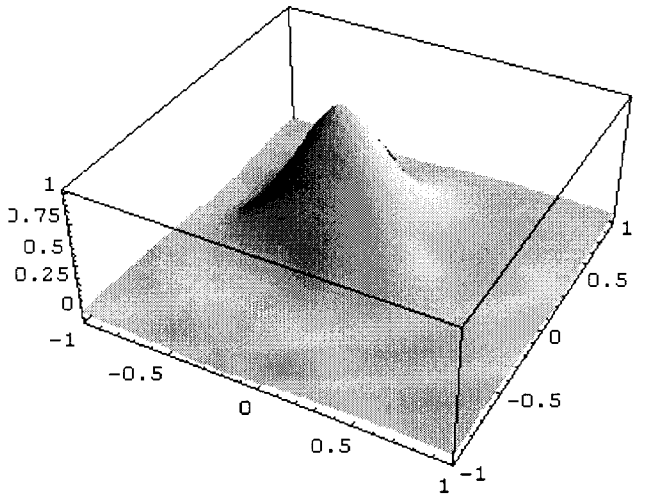

0.075	0.047	-0.752	0.047
0.296	-0.752	1.458	-0.752
0.075	0.047	-0.752	0.047
-0.020	0.075	0.296	0.075

Figure 6: Mirror membrane profile with a single actuator required to be at 1 μm (V/μm = 1.458), while all other actuators are set at zero displacement. The electric field values in V/μm required to achieve this membrane displacement profile are shown in the accompanying table.

4. FABRICATION TECHNIQUES

4.1 Transfer of Silicon Membranes

Wafer transfer techniques have been developed to transfer devices or thin films over other substrates [12-15]. Some of these techniques are capable of transferring thin-film microstructures, however the transfers were successful only in the case of small device sizes. Wafer-scale transfer techniques utilizing adhesives and/or molding materials have also been developed, [16-19]. Transfer techniques using sacrificial layers are not suitable for fabricating a wafer-scale continuous membrane, since the sacrificial layer under the continuous membrane needs to be completely etched away in order to complete the transfer. These techniques often result in generating residues around the transferred membrane surface. Therefore, we have developed a novel transfer technique for the fabrication of a continuous membrane deformable mirror, meeting the stringent optical quality requirements for future space telescopes [20].

Several silicon membranes, 4 inches in diameter, have been transferred using this process. The following briefly describes the fabrication sequence: A Silicon-On-Insulator (SOI) wafer and a silicon wafer are used as the carrier and electrode wafer, respectively. A 0.5 μm thick oxide is thermally grown on both sides of the wafers. Cr/Pt/Au metal layers are deposited and patterned on both wafers using a lift-off process. A 1 μm thick indium layer is then deposited on both wafers. Since the indium layer uniformly wets the Au layer, the Au "localizes" the In layer for subsequent hermetic bonding. This hermetic bonding process is a critical step prior to etching the SOI substrate wafer. A key problem is to prevent Indium from instantly oxidizing upon exposure to air, since the oxidized indium does not provide hermetic bonding. Thus, the indium deposition process is followed by the in-situ deposition of a 0.01 μm thick Au layer to prevent the indium surface oxidation problem. These deposited metal layers for bonding are also patterned using a lift-off process. The carrier wafer is subsequently bonded to the electrode wafer. An Electronic Vision aligner and a thermo-compression bonder are used to align and bond the two patterned wafers. The bonder chamber is pumped down to $1X10^{-5}$ Torr before bonding the two wafers. A piston pressure of 4 kPa is applied at 156 °C in a vacuum chamber to provide a complete hermetic sealing. The substrate of the SOI wafer is etched in a 25-wt % Tetramethylammonium hydroxide (TMAH) bath at 80 °C until the buried oxide is exposed. A Teflon fixture is used to protect the backside of the bonded wafers as well as their bonded interface. The exposed oxide is then

removed by using dilute hydrofluoric acid (49 % HF) droplets after an O_2 plasma ashing. O2 plasma is then used to remove any organic residues left on the membrane surface. The wafer-scale silicon membrane transfer process is complete at this stage. The surface figure of the transferred 10μm thick membrane is measured (after patterning and etching it into a small overhanging membrane. The measured peak-to-valley surface figure error of our membranes (area 1 mm^2) with indium posts spacing of 200 μm is approximately 9 nm. This surface figure error is mainly due to the "print-through" from the indium posts.

4.2 Thick-Film PZT Unimorph Fabrication

The capability for the deposition and patterning of PZT thick-films has been developed for integration into MEMS devices. For optimized room temperature piezoelectric response, PZT films with typical Zr:Ti ratios of 52:48 are used. As described above, the composition needs to be re-optimized for optimum operation at cryogenic temperatures. Films between 50 nm and ~8 μm can be deposited on 4" wafers using a sol-gel process by spin-coating the 2 – methoxyethanol-based precursor solution onto $Pt/Ti/SiO_2/Si$ substrates (Nova Electronic Materials), as shown in Figure 7.

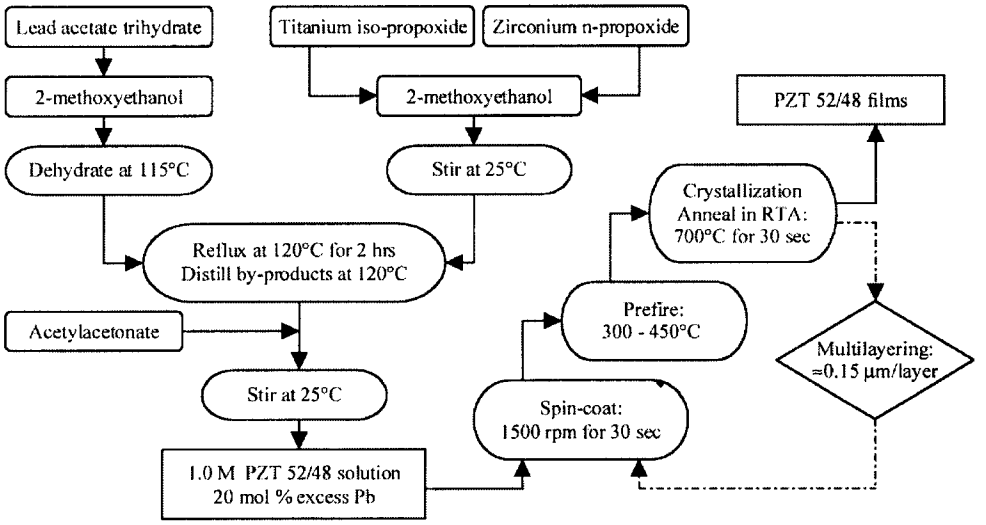

Figure 7: Processing scheme for thick PZT films. Edge bead removal is conducted prior to the crystallization step to avoid cracking of the deposit. A multiple layering process is employed for the deposition of thick films.

After the deposition of a single layer, the film is pyrolyzed to remove organics and heat-treated (typically at 700°C) to crystallize the film. Additional layers can then be spin-coated and heat-treated to increase the film thickness. It was found that in order to grow films thicker than ~3μm routinely on Si, it was necessary to remove the edge bead (from the spin coating process) from the wafer prior to pyrolysis and crystallization. Additional details on thick film processing are given elsewhere [23]. Figure 8 shows a cross-sectional scanning electron micrograph of a PZT film. The resulting films typically show dielectric constants of ~1000, loss tangents ~2 – 3%, remanent polarizations >20 $\mu C/cm^2$, and $e_{31,f}$ piezoelectric coefficients of –6.5 to –5 C/m^2. PZT films ~6 μm thick with similar properties have been used in MEMS accelerometers [21]. PZT films deposited on diaphragm structures with diameters of 500 μm, have resulted in center deflections of >3 microns for comparatively thin PZT films (~1.5 μm). For the larger stroke actuators required for this application, thicker PZT films would be required in order to increase the piezoelectric constant and the volume of the actuator material, thereby increasing the actuator stroke. While bulk PZT materials usually exhibit piezoelectric hysteresis, this problem is much reduced in thin films. This is because thin films show

much less non-180° domain wall motion (primary cause of hysteresis) than do even the hardest of bulk ceramics [22]. Also, it is well known that these extrinsic contributions to the piezoelectric response increase with film thickness, and decrease with decreasing temperature [22,24]. While domain wall motion been observed to lead to additional hysteresis in the electric field induced strain of thick films at room temperature, there is no available data in the literature on how rapidly these extrinsic contributions freeze out in thin films. Thus, an important direction of future research will be to determine how extrinsic contributions to the piezoelectric constant evolve as a function of film thickness at the low operating temperatures required for this application.

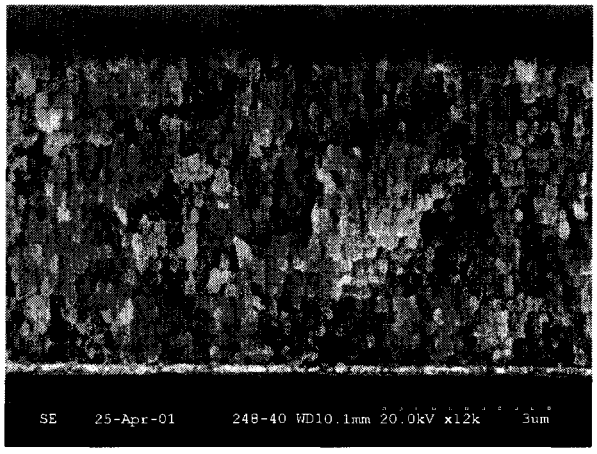

Figure 8: Cross-sectional micrograph of PZT thick film

5. FUTURE WORK

Fabrication of a piezoelectrically actuated MEMS mirror will be pursued. An optically polished silicon wafer will be used as a carrier wafer, and a flexible mirror membrane material will be subsequently deposited on it. An optical quality, deformable membrane mirror will be obtained by using the membrane material deposited on an optically polished carrier wafer, essentially making the transferred membrane surface a replica of the surface of the carrier wafer. Several membrane materials including polymers will be tested in order to select a mirror membrane material with optimized surface quality, mechanical compliance, stability, and frequency response. The selected membrane will be transferred to our piezoelectric unimorph actuator array or if necessary, onto other actuators operating on a different actuation mechanism. The microfabricated deformable mirror will be characterized with a full aperture measurement, which allows both interferometry and wavefront sensing measurements to be made.

6. CONCLUSIONS

The design, modeling and fabrication of large-stroke piezoelectric unimorph deformable mirror are described. The deformable mirror device consists of a "transferred" continuous membrane mirror supported by individually moving unimorph actuators. This membrane transfer approach is compatible with other actuation mechanisms (e.g. such as conventional actuators) as well. An actuator technique based on thick-film piezoelectric films is being developed for producing arrays of high-density unimorph actuators. The performance of piezoelectric unimorph membrane based actuators has been optimized via mathematical modeling. The deformable mirror concept described in this paper will support the requirements of several future space missions. The membrane transfer technology development is capable of producing optical quality surface figure for a wide range of deformable mirrors with apertures up to 250 mm. Development of the MEMS based large-stroke actuator technology is a new capability that is expected to benefit all missions that require precision miniature devices in a broad range of operational environments. The development path for this novel technology includes verification of performance on ground-based telescopes, diffraction-limited imaging systems, and laser communications systems.

ACKNOWLEDGEMENTS

The authors would like to thank Dr. Thomas George for his valuable comments. The Jet Propulsion Laboratory, California Institute of Technology carried out the research described in this paper under a contract with the National Aeronautics and Space Administration.

REFERENCES

1. R. Dekany, *et al.*, "Advanced Segmented Silicon Space Telescopes (ASSiST)," SPIE Int'l symp. On Astronomical Telescopes and Instrumentation, Adaptive Optical System Technologies II, 22-28 August 2002, Waikoloa, Hawaii, USA.
2. M. A. Ealey and J. F. Washeba, "Continuous Face Sheet Low Voltage Deformable Mirrors," *Optical Eng., 29,* p. 1191, Oct. 1990.
3. V. M. Bright et al., "Surface Micromachined Micro-Opto-Electro-Mechanical Systems," *IEICE Trans. Electron, E80-C (2)*, pp. 206-213, Feb. 1997.
4. W. D. Cowan et al., "Evaluation of Microfabricated Deformable Mirror Systems," *SPIE Conf. On Adaptive Optical System Technology*, Kona, Hawaii, March 1998, pp. 790-804.
5. G. Vdovin, "Optimization-based Operation of Micromachined Deformable Mirrors," *SPIE Conf. On Adaptive Optical System Technology*, Kona, Hawaii, March 1998, pp. 902-909.
6. P. K. C. Wang, et al., "A Method for Designing Electrostatic-Actuator Electrode Pattern in Micromachined Deformable Mirrors," *Sensors and Actuators A, 55*, pp.211-217, 1996.
7. T. Bifano et al., "Continuous-Membrane Surface-Micromachined Silicon Deformable Mirror," *Opt. Eng. 36 (5)*, p.1354 May 1997.
8. J. Mansell et al., "Silicon Deformable Mirrors and CMOS-based Wavefront Sensors," *SPIE International Conference, High-Resolution Wavefront Control*, San Diego, USA, Aug., 2000, pp. 15-25.
9. http://www.memsoptical.com/prodserv/products/def_mirrors.htm
10. P.Muralt, Integrated Ferroelectrics, 1999.
11. S. G. Kim *et al.,* Proc. Asia Display, 1998, pp. 329-334.
12. H. Nguyen *et al.*, "A Substrate-Independent Wafer Transfer Technique for Surface-Micromachined Devices," *IEEE Proc. MEMS '00, Sendai, Japan,* 2000.
13. T.E. Bell and K.D.Wise, "A Dissolved Wafer Process using a Porous Silicon Sacrificial Layer and a Lightly-Doped Bulk Silicon Etch-Stop," *IEEE Proc. MEMS '98*, Heidelberg, Germany, pp. 251-256, 1998.
14. C. G. Keller and R. T. Howe, "Hexile Tweezers for Teleoperated Micro-Assembly," *IEEE Proc. MEMS '97*, Nagoya, Japan, pp. 72-77, 1997.
15. A. Singh, *et al.*, "Batch Transfer of Microstructures using Flip-Chip Solder Bonding," *IEEE Journal of Microelectromechanical Systems*, pp. 27-33, 1999.
16. K. F. Harsh, *et al.*, "Flip-Chip Assembly for Si-Based RF MEMS," *IEEE Proc. MEMS '99*, Orlando, Florida USA, pp.273-278, 1999.
17. T. Akiyama, *et al.*, "Wafer-and Piece-Wise Si Tip Transfer Technologies for Applications in Scanning Probe Microscopy," *IEEE Journal of Microelectromechanical Systems*, pp. 65-70, 1999.
18. F. Niklaus, *et al.*, "Low-Temperature Wafer-Level Transfer Bonding," Journal of Microelectromechanical Systems, vol. 10, no. 4, pp. 525-531, 2001.
19. F. Niklaus, *et al.*, "Wafer-Level Membrane Transfer Bonding of Polycrystalline Silicon Bolometers for Use in Infrared Focal Plane Arrays," Journal of Micromechanics and Microengineering, vol. 11, pp. 509-503, 2001.
20. E. H. Yang and Dean V. Wiberg, "A New Wafer-Level Membrane Transfer Technique for MEMS Deformable Mirrors," *IEEE Micro Electro Mechanical Systems (MEMS) 2001 Conference*, Switzerland, 2000, pp. 80-83.
21. L. P. Wang, K. Deng, L. Zou, R. Wolf, R. J. Davis, and S. Trolier-McKinstry, "Microelectromechanical Systems (MEMS) Accelerometers Using Lead Zirconate Titanate Thick Films," *IEEE Electron Device Letters, 23 (4)*, pp. 182–184, 2002.
22. F. Xu, S. Trolier-McKinstry, W. Ren, and B. Xu, "Domain Wall Motion and its Contribution to the Dielectric and Piezoelectric Properties of Lead Zirconate Titanate Films," *J. Appl. Phys. 89 (2)* 1336-1348 (2001).
23. Q.F. Zhou, E. Hong, R. Wolf, and S. Trolier-McKinstry, "Dielectric and Piezoelectric Properties of PZT 52/48 Thick Films with (100) and Random Crystallographic Orientation," CC11.7 in *Mat. Res. Soc. Symp. Proc. 655 Ferroelectric Thin Films IX*, ed. by P. C. McIntyre, S. R. Gilbert, Y. Miyasaka, R. W. Schwartz, and D. Wouters, Materials Research Society, Warrendale, PA 2001
24. X. L. Zhang, Z. X. Chen, L. E. Cross, and W. A. Schulze, *J. Mater. Sci. 18*, 968, 1983.